Extended Object Tracking based on Set-Theoretic and Stochastic Fusion

Marcus Baum and **Uwe D. Hanebeck**
Intelligent Sensor-Actuator-Systems Laboratory (ISAS),
Institute for Anthropomatics,
Karlsruhe Institute of Technology (KIT), Germany.
marcus.baum@kit.edu, uwe.hanebeck@ieee.org

Abstract

In this paper, a novel approach for estimating the position and extent of an extended target is presented. In contrast to existing approaches, no statistical assumptions about the location of the measurement sources on the extended target object are made. As a consequence, a combined set-theoretic and stochastic estimator is obtained that is robust to systematic errors in the target model. The applicability of the new approach is demonstrated by means of circular shapes.

Index Terms

Tracking, extended objects, random sets, estimation.

I. Introduction

The standard target tracking problem considers the tracking of a point source based on noisy measurements. In doing so, it is assumed that the object extension is negligible in comparison to the sensor noise. If this is not the case, target tracking algorithms have to take into account that measurements may stem from different locations on the extended target object. A major difficulty is that the extent of the target object is unknown and has to be estimated in addition to the position of the target. Scenarios for tracking extended objects often occur in military surveillance with radar devices [1], [2]. For instance, a modern high-resolution radar device may receive measurements from different scattering centers, called measurement sources, on the extended target. Such a scenario is depicted in Figure 1, where several measurement sources per time step are resolved on an aircraft. The measurements themselves are noisy observations of these measurement sources. The stochastic measurement noise stems from the particular sensor, e.g., of a radar device, and its statistics are usually given. However, the locations of the measurement sources are typically unknown. Extended object tracking methods are also useful for group target tracking [2] when resolution conflicts make it impossible to track each single group member (see Figure 1).

A. Related Work

In [3]–[5], the target extent is modeled by means of a spatial distribution, i.e., each measurement source is an independent random draw from a target-dependent probability distribution. Spatial distribution models have been used in combination with *Probability Hyptheses Density (PHD)* filters [6], [7] and in [8] spatial cluster processes are used for extended object tracking. In [2], [9], an elliptic target extent is modeled with a random matrix that is treated as an additional state variable. The random matrix approach has also been embedded into the *Probabilistic Multiple Hypotheses Tracker (PMHT)* framework [10] in order to track multiple extended objects. In [11]–[14], a so-called Random Hypersurface Model (RHM), which assumes that each single measurement source lies on a scaled version of the target boundary, is used for tracking elliptic and star-convex shapes. An approach for tracking the shape of contaminant clouds is introduced in [15] and down-range extent measurements are used for instance in [16] for tracking an extended object.

B. Contributions

In many scenarios, it is unreasonable to place any (statistical) restriction on the measurement sources. For instance, when tracking an aircraft formation, the behavior of a single formation member is nearly unpredictable due to the high complexity of the group behavior. It is therefore difficult to determine a reasonable probability distribution for the measurement sources. Furthermore, consider the tracking of a ship with a high-resolution radar device. Due to the complex character of the surface of the ship, it is unpredictable which scattering center on the ship is responsible for a particular measurement. Existing methods for tracking extended objects are not able to incorporate this lack of knowledge and certainly, wrong assumptions on the measurement sources may lead to poor estimation results.

The novel approach presented in this article makes *no* assumption about the measurement sources on the extended object. In particular no statistical assumptions are made. The only utilized information about a measurement source is that it lies on the extended target object. As a consequence, the resulting estimator is robust to systematic errors in the target model, i.e., when the true shape and distribution of the measurement sources do not coincide with the modeled target, and is thus able to supply more precise estimation results than standard approaches. At this point, it is important to note that the measurement noise itself is still assumed to be stochastic. Hence, the uncertainty about the measurement sources is modeled as a set and the measurement error is assumed to be stochastic.

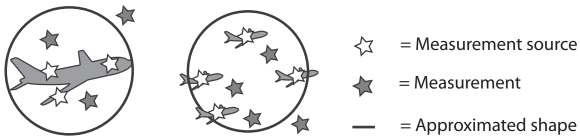

Fig. 1: Scenarios: Extended object (left) and group target (right).

A consequence of this set-theoretic target model is that the scaling of the extended object cannot be estimated only by means of noisy position measurements. In order to estimate the size of the extended object one has to incorporate further knowledge. In this paper, we assume that the number of measurements received at a time step depends on the scaling of the extended object.

C. Structure

The remainder of this paper is structured as follows: After a detailed problem description in Section II, we first restrict the problem in Section III to a static extended object, i.e., a non-moving target with unknown but fixed location and extent. First, we consider the case of known extent, i.e., the radius of the smallest enclosing circle of the target object is given. The second step is to construct an estimator for both the location and radius of the extended object. To this end, a novel outer-bounding technique based on hyperboloids is developed. It turns out that it is necessary to incorporate further statistical information in order to estimate the radius of the smallest enclosing disc. In particular, it is assumed here that the number of measurements received per time step depends on the size of the object. Details are explained in Section IV and Section V, where the instantaneous tracking of an extended object whose position and shape changes with time is discussed. The applicability and advantages of the new approach are shown by means of experiments in Section VI.

This paper is an extended and revised version of the conference paper [17], where the basic idea of combined set-theoretic and stochastic approach was first introduced for circular discs. The approach has been applied for tracking axis-aligned rectangles in [18].

II. Problem Setup

We treat the problem of tracking an extended target object based on noisy position measurements stemming from the target surface. The target extent is modeled in this paper as a basic geometric shape, i.e., a circular disc. We assume that the extended target is enclosed at each time step k by a circular shape

$$\mathbf{K}(\underline{\tilde{p}}_k) = \{[x, y]^T \in \mathbb{R}^2 \,|\, (x - \tilde{x}_k^c)^2 + (y - \tilde{y}_k^c)^2 \leq \tilde{r}_k^2\} \quad ,$$

where $\underline{\tilde{p}}_k = [\tilde{x}^c, \tilde{y}^c, \tilde{r}]^T$ consists of the center and radius of the circle.

We aim at estimating the parameter vector $\tilde{\underline{p}}_k$, which is not directly observable. Instead, at each time step k, a finite set of two-dimensional Cartesian position measurements $\{\hat{\underline{z}}_{k,j}\}_{j=1}^{n_k}$ is available. Each of these individual measurements $\hat{\underline{z}}_{k,j}$ is the noisy observation of a two-dimensional point $\tilde{\underline{z}}_{k,j}$, named measurement source, which is known to lie in $\mathbf{K}(\tilde{\underline{p}}_k)$, i.e.,

$$\hat{\underline{z}}_{k,j} = \tilde{\underline{z}}_{k,j} + \underline{\boldsymbol{w}}_{k,j} \text{ and } \tilde{\underline{z}}_{k,j} \in \mathbf{K}(\tilde{\underline{p}}_k) \ , \tag{1}$$

where $\underline{\boldsymbol{w}}_{k,j}$ denotes two-dimensional additive white observation noise[1] that models a random Cartesian displacement. The probability distribution of the measurement noise $\underline{\boldsymbol{w}}_{k,j}$ is assumed to be known. The measurement source $\tilde{\underline{z}}_{k,j}$ is not known, so that we do not know which point on the extended object was actually measured by $\hat{\underline{z}}_{k,j}$. Note that the measurement sources $\tilde{\underline{z}}_{k,j}$ on the extended object are not assumed to be drawn from a particular probability distribution. Hence, the measurement model suffers from both a set-valued uncertainty *and* a stochastic uncertainty. All told, this is not a classical state estimation problem, because the hidden state is connected to the observable state with a (random) many-to-many relation. For each given circular disc, there is a *(random) set* of possible measurements. On the other hand, in classical state estimation, the hidden state is related to an observable state by a (random) function defined by the measurement equation.

The position as well as the shape of the extended object may vary over time. The temporal evolution of the (smallest) circular disc, which includes the extended object, is modeled by means of a so-called *extended motion model* that captures both the motion and the extent of the target object (details are given in Section IV).

III. Static Extended Objects

In this section, we concentrate on a static extended object, i.e., an extended object whose smallest enclosing circle neither moves nor changes its radius over time. Then, the fixed but unknown parameter vector $\tilde{\underline{p}}$ of the extended object $\mathcal{O}(\tilde{\underline{p}})$ is to be estimated. For the sake of simplicity, we assume that at each time step k, a single position measurement $\hat{\underline{z}}_k$ is given.

A. Circular Discs with Known Radius

In the following, a combined set-theoretic and stochastic estimator for the center of a circular disc with known radius is constructed. Hence, the true radius $\tilde{r}$ of the smallest enclosing circle of the target object is given and only the unknown center $[\tilde{x}^c, \tilde{y}^c]^T$ is desired. According to Equation (1), we obtain the measurement equation

$$\hat{\underline{z}}_k = [\tilde{x}^c, \tilde{y}^c]^T + \underline{e}_k + \underline{\boldsymbol{w}}_k \ , \tag{2}$$

[1]Note that all random variables are printed bold face in this paper.

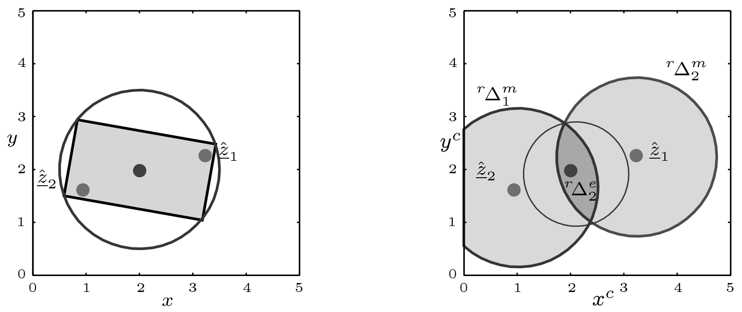

(a) A rectangular extended object and its smallest enclosing circle. Two position measurements $\hat{\underline{z}}_1$ and $\hat{\underline{z}}_2$ have been received.

(b) Intersection of the measurement solution sets for $\hat{\underline{z}}_1$ and $\hat{\underline{z}}_2$. The intersection can be bounded by a circle.

Fig. 2: Set-theoretic estimation of the center of the smallest enclosing circle of an extended object with known radius.

where $\underline{e}_k \in \mathbf{K}(0, 0, \tilde{r})$ (note that $\underline{e}_k := \hat{\underline{z}}_k - [\tilde{x}^c, \tilde{y}^c]^T$). This measurement equation maps the parameters $[\tilde{x}^c, \tilde{y}^c]^T$ to the measurement $\hat{\underline{z}}_k$, where $\underline{\boldsymbol{w}}_k$ is Gaussian measurement noise and $\underline{e}_k$ is an unknown but bounded error.

Equation (2) is equivalent to $[\tilde{x}^c, \tilde{y}^c]^T \in \mathbf{K}([\hat{\underline{z}}_k - \underline{\boldsymbol{w}}_k, \tilde{r}]^T)$. For this reason, all possible centers $[\tilde{x}^c, \tilde{y}^c]^T$ that are consistent with measurement $\hat{\underline{z}}_k$ are an element of a circular disc with random center $\hat{\underline{z}}_k - \underline{\boldsymbol{w}}_k$ and given radius $\tilde{r}$. The set of all possible centers is called *measurement solution set* and denoted with ${}^r\Delta_k^m := \mathbf{K}(\hat{\underline{z}}_k - \underline{\boldsymbol{w}}_k, \tilde{r})$. [2]

Example 1. In Figure 2a, an extended object with a rectangular shape is shown. The true circular disc whose location is to be estimated is drawn and the first two measurements $\hat{\underline{z}}_1$ and $\hat{\underline{z}}_2$ are depicted (we assumed noise-free measurements, i.e., $\underline{\boldsymbol{w}}_1 = 0$ and $\underline{\boldsymbol{w}}_2 = 0$). The parameter space consisting of the location of the true disc is shown in Figure 2b. The measurement solution sets ${}^r\Delta_1^m$ and ${}^r\Delta_2^m$ of the two measurements are circular discs. These sets consist of all feasible locations that enclose the corresponding measurement. Since $\hat{\underline{z}}_1$ and $\hat{\underline{z}}_2$ both lie in the true circular disc, the true location is an element of ${}^r\Delta_2^e ={}^r \Delta_1^m \cap^r \Delta_2^m$. Note that ${}^r\Delta_2^e$ is not a circular disc again.

All told, each measurement $\hat{\underline{z}}_k$ yields a random set for the state ${}^r\Delta_k^m$. A recursive fusion procedure for the random sets ${}^r\Delta_k^m$ is given by a so-called combined set-theoretic and stochastic estimator (see [19]–[23] for a detailed description).

A combined set-theoretic and stochastic estimator represents the uncertainty about the tstate at time step k with a random set ${}^r\Delta_k^e$ (called solution set). At each time step k, a new random set ${}^r\Delta_k^m$

[2]The superscript r in ${}^r\Delta_k^m$ emphasizes that the radius is known.

becomes available (constructed from the measurement), which has to be fused with the prior random set ${}^r\Delta^e_{k-1}$. A natural fusion rule for random sets is intersection (conditioned on non-emptiness), i.e., the updated solution set becomes ${}^r\Delta^e_k ={}^r \Delta^e_{k-1} \cap^r \Delta^m_k$. The exact recursive computation of ${}^r\Delta^e_k$ can be difficult and time consuming. Hence, in order to allow a fast recursive computation, the sets ${}^r\Delta^e_k$ are usually outer-bounded with supersets that can be described with a (fixed) number of parameters such as ellipsoids [24].

In this particular case, it is suitable to bound the true solution set ${}^r\Delta^e_k$ with a circular disc again (see Figure 2b). In doing so, whenever a new measurement is received, the intersection of the corresponding measurement solution set and the current solution set has to be bounded with a (smallest) circular disc. Note that the detailed formulas turn out to be a special case of the general problem and can be found in Remark 3.

Remark 1. Combined set-theoretic and stochastic estimators are a well-known concept in state estimation, where one has to deal with both stochastic and bounded errors [19]–[23]. It is worth mentioning that combined stochastic and set-theoretic filters turn into a pure set-theoretic filter if the stochastic noise vanishes. Furthermore, if the bounded noise error is zero, a stochastic filter is obtained. The fusion of random sets by means of set intersection can also be interpreted as the Dempster-Shafer rule of combination. Furthermore, the measurement solution set can be seen as a generalized measurement as described by Mahler in [25].

B. Circular Discs with Unknown Radius

In the following, the goal is to estimate the location of a static extended object with an unknown but fixed radius. Thus, the estimator has to simultaneously consider all possible radii. Consider a particular measurement $\hat{\underline{z}}_k = [x^m_k, y^m_k]^T$ at time step k. Each parameter vector $[x^c, y^c, r]^T$ specifying a circular disc that encloses $\hat{\underline{z}}_k$ satisfies the condition $\hat{\underline{z}}_k - \underline{\boldsymbol{w}}_{k,j} \in \mathbf{K}(x^c, y^c, r)$. Hence, for a given measurement $\hat{\underline{z}}_k$, the set of all possible parameter vectors can be restricted to

$$\Delta^m_k := \left\{[x^c, y^c, r]^T \in \mathbb{R}^3 \mid \quad ||[x^c, y^c]^T - (\hat{\underline{z}}_k - \underline{\boldsymbol{w}}_k)||^2_2 \leq r^2\right\} . \tag{3}$$

In fact, Δ^m_k is a random cone in three-dimensional space, which is oriented along the r-axis with apex $\hat{\underline{z}}_k - \underline{\boldsymbol{w}}_k$ in the xy-plane and perpendicular cone angle.

Example 2. In Figure 3a, the extended object with a rectangular shape is shown again (but now the radius is unknown as well). Furthermore, the first two (noise-free) sample measurements $\hat{\underline{z}}_1$ and $\hat{\underline{z}}_2$ are depicted. The bounds of the corresponding cones Δ^m_1 and Δ^m_2 in the parameter-space are shown in Figure 3b. The entire sets Δ^m_1 and Δ^m_2 are given by all points that lie “above” the plotted bounds. Since $\hat{\underline{z}}_1$ and $\hat{\underline{z}}_2$ both lie in the circular disc, the parameters are elements of $\Delta^e_2 = \Delta^m_1 \cap \Delta^m_2$. Figure 3c and 3d illustrate an example of the solution set Δ^e_4 for four received measurements. The

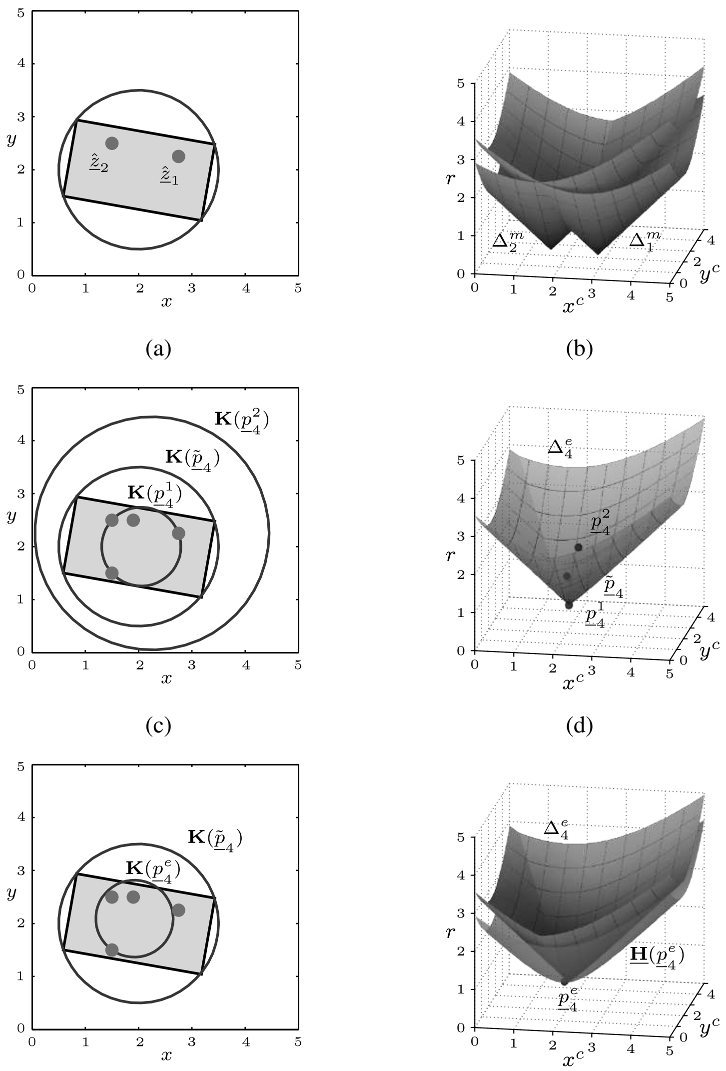

(a) (b) (c) (d) (e) (f)

Fig. 3: Set-theoretic estimation of an extended object.

discs $\mathbf{K}(\tilde{\underline{p}}_4), \mathbf{K}(\underline{p}_4^1)$ and $\mathbf{K}(\underline{p}_4^2)$ are examples for feasible circular discs. $\mathbf{K}(\underline{p}_4^1)$ represents the smallest enclosing circle of the given measurements. In this example, $\mathbf{K}(\tilde{\underline{p}}_4)$ is the true disc, since it represents the smallest enclosing circle of the target object. In Figure 3d, the bound of the set Δ_4^e and the parameters of the example discs are depicted. Furthermore, the corresponding parameters $\tilde{\underline{p}}_4, \underline{p}_4^1$ and $\underline{p}_4^2$ of the example discs (see Figure 3c) are marked. Note that Δ_4^e is neither a cone nor any other basic geometric object.

The exact recursive computation of the random set $\Delta_k^e = \Delta_{k-1}^e \cap \Delta_k^m$ is computationally intractable. Unfortunately, there is in general no proper parametric description of the solution set Δ_k^e. Note that the intersection of two cones in the form of Equation (3) is not a cone again. In order to tackle this problem, we introduce a novel outer-bounding technique based on hyperboloids (see Figure 3e and Figure 3f). We make use of the fact that the intersection of a cone and a hyperboloid (see Definition 1) can be outer-bounded by a hyperboloid again. This approximation technique enables recursively approximating Δ_k^e with hyperboloids.

Definition 1 (Hyperboloid of Revolution)**.** The upper sheet of a two-sheeted circular hyperboloid of revolution is given by

$$\mathbf{H}(x^e, y^e, z^e, a) \;:=\; \left\{[x^c, y^c, r]^T \in \mathbb{R}^3 \mid r \geq z^e \text{ and } (x^c - x^e)^2 + (y^c - y^e)^2 + a^2 \leq (r - z^e)^2\right\}$$

with $x^e, y^e, z^e \in \mathbb{R}$ and $a \in \mathbb{R}^+$.

Remark 2. A hyperboloid $\mathbf{H}(x^e, y^e, z^e, a)$ has the following properties (see Figure 4a):

- the focus is $F = [x^e, y^e, z^e]^T$,
- the apex is located at $A = [x^e, y^e, a + z^e]^T$,
- the cone angle is orthogonal, and
- the hyperboloid is oriented along the r–axis.

Definition 2. A hyperboloid of the form $\mathbf{H}(x^e, y^e, 0, a)$ is abbreviated with $\underline{\mathbf{H}}(x^e, y^e, a)$. Furthermore, the set $\underline{\mathbf{C}}(x^e, y^e) := \mathbf{H}(x^e, y^e, 0, 0)$ is a cone oriented along the r–axis whose apex lies on the $x^c y^c$–plane.

Theorem 1 in the Appendix gives formulas for outer-bounding the intersection of a cone and hyperboloid with a hyperboloid. The theorem is based on the observation that the intersection of the bounds[3] $\partial\underline{\mathbf{H}}(\underline{p}_{k-1}^e)$ and $\partial\underline{\mathbf{C}}(\underline{\hat{z}}_k)$ is a hyperbola lying in a plane perpendicular to the $x^c y^c$-plane (see Figure 4). Based on Theorem 1, we can define a function $\mathcal{G}_1(\cdot)$ (see Definition 3 in the Appendix), which maps the parameters of the hyperboloid $\underline{\mathbf{H}}(\underline{p}_{k-1}^e)$ and a cone $\underline{\mathbf{C}}(\underline{\hat{z}}_k)$ to the parameters of the resulting hyperboloid bounding their intersection.

Equipped with these outer-bounding techniques, we can define a recursive combined set-theoretic and stochastic estimator, which uses random hyperboloids for expressing the uncertainty about the location of the circle (for each possible radius).

Set-Theoretic and Stochastic Estimator (SSTE) 1

- **Solution Set**
  Hyperboloid $\mathbf{H}(\underline{\boldsymbol{p}}_k^e)$ with $\underline{\boldsymbol{p}}_k^e = [\boldsymbol{x}_k^e, \boldsymbol{y}_k^e, \boldsymbol{a}_k^e]^T$ and $\underline{\boldsymbol{p}}_k^e \sim \mathcal{N}(\underline{p}; \hat{\underline{p}}_k^e, \mathbf{C}_k^e)$.
- **Measurement Solution Set**
  Cone $\underline{\mathbf{C}}(\underline{\boldsymbol{z}}_k)$ with $\underline{\boldsymbol{z}}_k := \underline{\hat{z}}_k - \underline{\boldsymbol{w}}_k$ and $\underline{\boldsymbol{z}}_k \sim \mathcal{N}(z; \underline{\hat{z}}_k, \mathbf{C}_k^z)$.

[3]The operator ∂ denotes the bound of a set.

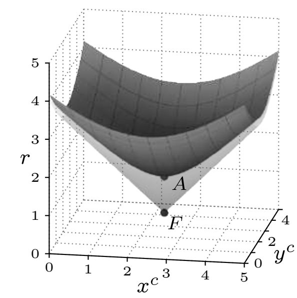

(a) A hyperboloid with apex A and focus F

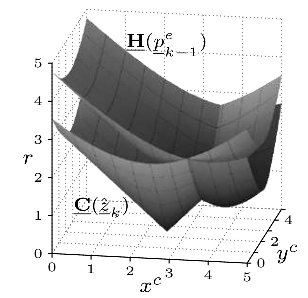

(b) A cone $\underline{\mathbf{C}}([2.5, 2]^T)$ and a hyperboloid $\underline{\mathbf{H}}([4, 2, 1]^T)$.

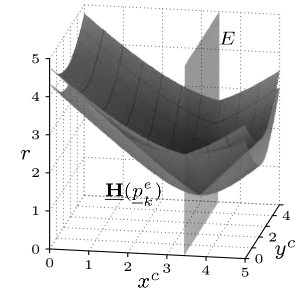

(c) Approximated intersection.

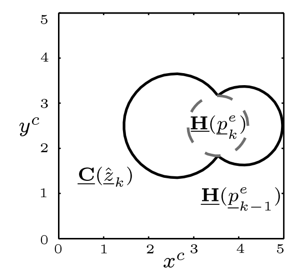

(d) $x^c y^c$-plane for $r = 1.8$.

Fig. 4: Approximating the intersection of a cone and a hyperboloid with a hyperboloid.

- **Fusion**

$$\underline{\boldsymbol{p}}^e_k = \mathcal{G}_1(\underline{\boldsymbol{z}}_k, \underline{\boldsymbol{p}}^e_{k-1}) \text{ and } \underline{\boldsymbol{p}}^e_1 = [\underline{\boldsymbol{z}}^T_1, 0]^T \tag{4}$$

The (nonlinear) function $\mathcal{G}_1(\cdot)$ in Equation (4) has to be evaluated stochastically, i.e., the arguments are random variables. In general, the distribution of $\underline{\boldsymbol{p}}^e_k$ cannot be computed in closed form for given distributions of $\underline{\boldsymbol{z}}_k$ and $\underline{\boldsymbol{p}}^e_{k-1}$, since $\mathcal{G}_1(\cdot)$ is a nonlinear function. Nevertheless, the distribution of $\underline{\boldsymbol{p}}^e_k$ can be approximated with a Gaussian distribution by employing the prediction step of a nonlinear stochastic state estimator such as the Gaussian Filter [26] and the UKF [27].

Remark 3. When the true radius is given, SSTE 1 turns into the SSTE for circular discs with known radius from Section III-A. The outer-bound of the two-dimensional random solution set ${}^r\boldsymbol{\Delta}^e_k$ for the desired center results from the random hyperboloid $\underline{\mathbf{H}}(\underline{\boldsymbol{p}}^e_k)$ and is given by $\mathbf{K}(\boldsymbol{x}^e_k, \boldsymbol{y}^e_k, \sqrt{(\tilde{r})^2 - (\boldsymbol{a}^e_k)^2})$ given that $\boldsymbol{a}^e_k \leq \tilde{r}$. If the true radius $\tilde{r}$ is known, the probability density function $f(\underline{p}^e_k)$ of $\underline{\boldsymbol{p}}^e_k$ in SSTE 1 can be restricted (at each time step) to feasible values by computing the posterior density $f(\underline{p}^e_k | \{\boldsymbol{a}^e_k \leq \tilde{r}\})$. Note that if $a^e_k > \tilde{r}$ there is no disc with radius $\tilde{r}$ in $\underline{\mathbf{H}}(\underline{p}^e_k)$. In this context, see also Figure 4d. The probability density $f(\underline{p}^e_k | \{\boldsymbol{a}^e_k \leq \tilde{r}\})$ is a truncated Gaussian distribution whose first two moments can be computed according to [28]. Hence, SSTE 1 consists of an SSTE for circular discs with given radius (see Section III-A) for each possible radius.

IV. Dynamic Extended Objects

In this section, we consider an extended object that moves and changes its shape over time. At each time step k, the parameters $\underline{\tilde{p}}_k$ of the smallest shape $\mathcal{O}(\underline{\tilde{p}}_k)$ that includes the true target shape are to be estimated. Now, at each time step k, a finite set of two-dimensional position measurements $\{\underline{\hat{z}}_k\}_{j=1}^{n_k}$ is available. Each of these individual measurements $\underline{\hat{z}}_k$ is the noisy observation of a measurement source $\underline{\tilde{z}}_{k,j}$ according to Equation (1).

In order to capture translations along the r-axis (which models the scaling of the extended object), it becomes necessary to represent solution sets with hyperboloids of the form $\mathbf{H}([x_k^e, y_k^e, z_k^e, a_k^e]^T)$ instead of $\underline{\mathbf{H}}([x_k^e, y_k^e, a_k^e]^T)$. For this purpose, throughout the rest of this paper, the parameter vector $\underline{\boldsymbol{p}}_k^e$ is of the form $[\boldsymbol{x}_k^e, \boldsymbol{y}_k^e, \boldsymbol{z}_k^e, \boldsymbol{a}_k^e]^T$.

The parameter vector $\underline{\boldsymbol{p}}_k^e$ is assumed to evolve according to a so-called extended motion model of the form

$$\underline{\boldsymbol{p}}_k^p = \begin{bmatrix} \mathbf{A}_k & 0 \\ 0 & 1 \end{bmatrix} \underline{\boldsymbol{p}}_{k-1}^e + \begin{bmatrix} \mathbf{B}_k \\ 0 \end{bmatrix} (\underline{\hat{u}}_{k-1} + \underline{\boldsymbol{v}}_{k-1}) + \begin{bmatrix} 0 & 0 & d_k & 0 \end{bmatrix}^T \tag{5}$$

that maps the parameter vector $\underline{\boldsymbol{p}}_{k-1}^e$ at time step $k-1$ to the predicted parameters $\underline{\boldsymbol{p}}_k^p$ at time step k. The random vector $\underline{\boldsymbol{v}}_{k-1}$ models input noise and $\underline{\hat{u}}_{k-1}$ denotes the deterministic system input. The term d_k shifts the hyperboloid along the z-axis in order to capture a set-theoretic system error on the circle center. This model corresponds to a linear motion of the center corrupted by additive Gaussian noise and a set-theoretic error. Based on this dynamic model, SSTE 1 can be extended to the dynamic case.

Set-Theoretic and Stochastic Estimator (SSTE) 2

- **Solution Set**

  Hyperboloid $\mathbf{H}(\underline{\boldsymbol{p}}_k^e)$ with $\underline{\boldsymbol{p}}_k^e \sim \mathcal{N}(\underline{p}; \underline{\hat{p}}_k^e, \mathbf{C}_k^e)$.
- **Measurement Solution Set**

  The measurements $\{\underline{\hat{z}}_{k,j}\}_{j=1}^{n_k}$ yield $\underline{\mathbf{C}}(\underline{\boldsymbol{z}}_{k,0}), \ldots, \underline{\mathbf{C}}(\underline{\boldsymbol{z}}_{k,n_k})$ with $\underline{\boldsymbol{z}}_{k,j} := \underline{\hat{z}}_{k,j} - \underline{\boldsymbol{w}}_{k,j}$ (for all j).
- **Prediction**

  Compute the $\underline{\boldsymbol{p}}_k^p$ based on the estimate $\mathbf{H}(\underline{\boldsymbol{p}}_{k-1}^e)$. (see Equation (5)).
- **Fusion**

  $\mathbf{H}(\underline{\boldsymbol{p}}_k^e)$ is the result of outer-bounding $\bigcap_j \underline{\mathbf{C}}(\underline{\boldsymbol{z}}_{k,j}) \cap \mathbf{H}(\underline{\boldsymbol{p}}_k^p)$ (with $\underline{\boldsymbol{p}}_1^p = [\underline{\boldsymbol{z}}_1^T, 0, 0]^T$). With $\underline{\boldsymbol{p}}_{k,0}^e := \underline{\boldsymbol{p}}_k^p$ and $\underline{\boldsymbol{p}}_{k,j}^e = \mathcal{G}_2(\underline{\boldsymbol{p}}_{k,j-1}^e, \underline{\boldsymbol{z}}_{k,j})$ one obtains $\underline{\boldsymbol{p}}_k^e := \underline{\boldsymbol{p}}_{k,n_k}^e$.

A proper function $\mathcal{G}_2(\cdot)$ (see Definition 4) for the fusion step in SSTE 2 can be constructed by means of Theorem 2, which is actually an extension of Theorem 1 to hyperboloids translated along the r-axis. Theorem 2 is based on the observation that the intersection of $\partial\underline{\mathbf{C}}(\underline{\hat{z}}_{k,j})$ and $\partial\mathbf{H}(\underline{p}_{k,j-1}^e)$

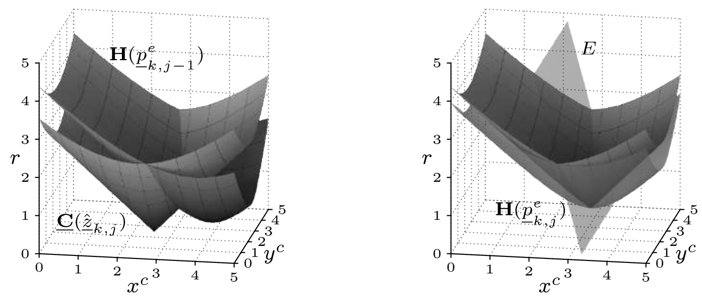

(a) Cone $\underline{\mathbf{C}}([2.5, 2]^T)$ and hyperboloid $\mathbf{H}([4, 2, -0.5, 1]^T)$.

(b) Approximated intersection.

Fig. 5: Approximating the intersection of a cone and a hyperboloid with a hyperboloid.

is a hyperbola lying in a plane (see Figure 5). In contrast to Theorem 1, this plane does not have to be perpendicular to the $x^c y^c$-plane.

Remark 4. In analogy to Remark 3, when the true radius is given at time step k, SSTE 2 turns into a SSTE for circular discs with known radius. The outer-bound of the two-dimensional random solution set ${}^r\boldsymbol{\Delta}^e_k$ for the desired center results from the random hyperboloid $\mathbf{H}(\underline{\boldsymbol{p}}^e_k)$ and is given by $\mathbf{K}(\boldsymbol{x}^e_k, \boldsymbol{y}^e_k, \sqrt{(\tilde{r})^2 - (\boldsymbol{a}^e_k + \boldsymbol{z}^e_k)^2})$ given that $\boldsymbol{a}^e_k + \boldsymbol{z}^e_k \leq \tilde{r}$. If the true radius $\tilde{r}$ is known, the probability density function $f(\underline{p}^e_k)$ of $\underline{\boldsymbol{p}}^e_k$ in SSTE 2 can be restricted (at each time step) to feasible values by computing the posterior density $f(\underline{p}^e_k | \{\boldsymbol{a}^e_k + \boldsymbol{z}^e_k \leq \tilde{r}\})$. Note that if $a^e_k + \boldsymbol{z}^e_k > \tilde{r}$ there is no disc with radius $\tilde{r}$ in $\mathbf{H}(\underline{p}^e_k)$.

V. Incorporating Further Knowledge about the Rradius

So far, we have assumed that the radius is unknown. Unfortunately, it is not possible to estimate the radius without further modeling assumptions. In this work, we infer the radius based on the number of measurements received at a time step.

A realistic assumption, which is often satisfied in scenarios for extended object tracking, is that the number of measurements received from the target object at a particular time step depends on its size. For instance, [2] suggests a Poisson distribution with an expectation proportional to the area of the extended target. Here, we assume that a conditional probability density $f(n_k | r_k)$, which specifies the number of measurements depending on the current radius of the extended object is available. This assumption is justified since the radius is proportional to the perimeter of a circular disc. It would also be possible to consider the area of the extended object, instead of the perimeter. However, this would result in nonlinear constraints.

In order to incorporate statistical information about the radius into SSTE 2, we maintain an additional random variable $\boldsymbol{r}^e_k$ that captures the knowledge about the true radius obtained from the number of measurements n_k. Hence, the state vector at time step k is given by the random vector $[(\underline{\boldsymbol{p}}_k^e)^T, \boldsymbol{r}_k^e]^T$. The estimate $[(\underline{\boldsymbol{p}}_{k-1}^e)^T, \boldsymbol{r}_{k-1}^e]^T$ at time step $k-1$ can be propagated through the extended motion model according to

$$\begin{bmatrix} \underline{\boldsymbol{p}}_k^p \\ \boldsymbol{r}_k^p \end{bmatrix} = \begin{bmatrix} \mathbf{A}_k & 0 & 0 \\ 0 & 1 & 0 \\ 0 & 0 & 1 \end{bmatrix} \cdot \begin{bmatrix} \underline{\boldsymbol{p}}_{k-1}^e \\ \boldsymbol{r}_{k-1}^e \end{bmatrix} + \begin{bmatrix} \mathbf{B}_k \\ 0 \\ b_k^{(3)} \end{bmatrix} (\hat{\underline{u}}_{k-1} + \underline{\boldsymbol{v}}_{k-1}) \ ,$$

where $b_k^{(3)}$ denotes the third row of $\mathbf{B}_k$. Again, we assume that $[(\boldsymbol{p}_{k-1}^e)^T, \boldsymbol{r}_{k-1}^e]^T$ is Gaussian distributed such that $[\underline{\boldsymbol{p}}_k^p, \boldsymbol{r}_k^p]^T$ is also Gaussian distributed and can be computed with the Kalman filter formulas for the prediction step.

The prediction $[(\underline{\boldsymbol{p}}_k^p)^T, \boldsymbol{r}_k^p]^T$ can be updated with $\{\hat{\underline{z}}_{k,j}\}_{j=1}^{n_k}$ in order to obtain the posteriori pdf of $[(\underline{\boldsymbol{p}}_k^e)^T, \boldsymbol{r}_k^e]^T$ (given n_k) in the following way:

1) Starting with $\underline{\boldsymbol{p}}_{k,0}^e := \underline{\boldsymbol{p}}_k^p$ the probability distribution $f(\underline{p}_k^e, r_k^e)$ of $[(\underline{\boldsymbol{p}}_k^e)^T, \boldsymbol{r}_k^e]^T := [(\underline{\boldsymbol{p}}_{k,n_k}^e)^T, \boldsymbol{r}_k^e]^T$, where $\underline{\boldsymbol{p}}_{k,j}^e := \mathcal{G}_2(\underline{\boldsymbol{z}}_{k,j}, \underline{\boldsymbol{p}}_{k,j-1}^e)$ for $1 \leq j \leq n_k$ can be computed recursively by means of a nonlinear state estimator. This step recursively intersects the cones resulting from the measurements (see SSTE 2).
2) Incorporate the information about the radius by computing the posterior density $f(\underline{p}_k^e, r_k^e \mid n_k)$ with Bayes' rule
$$f(\underline{p}_k^e, r_k^e \mid n_k) = c \cdot f(n_k \mid r_k) \cdot f(\underline{p}_k^e, r_k^e) \ ,$$
where c is a normalization constant.
3) Compute the posterior density
$$f(\underline{p}_k^e, r_k^e \mid n_k, \{\boldsymbol{a}_k^e + \boldsymbol{z}_k^e \leq \boldsymbol{r}_k^e\})$$
what corresponds to truncating infeasible values. This constraint arises from the fact that if $\boldsymbol{a}_k^e + \boldsymbol{z}_k^e > \boldsymbol{r}_k^e$, there is no disc with radius $\boldsymbol{r}_k^e$ in $\underline{\mathbf{H}}(\underline{p}_k^e)$. Formulas for approximating a truncated Gaussian with a Gaussian again are given in [28].

A proper point estimate for the radius is given by $\mathrm{E}[\boldsymbol{r}_k^e]$ and a point estimate for the center is given by $\mathrm{E}[[\boldsymbol{x}_k^e, \boldsymbol{y}_k^e]^T]$ and covariance matrix $\mathrm{Cov}[[\boldsymbol{x}_k^e, \boldsymbol{y}_k^e, \boldsymbol{r}_k^e]^T]$. Note that if $\boldsymbol{r}_k^e$ is given, the special case of known radius is obtained (see Remark 3).

The convergence behavior of the above introduced estimator needs further discussion. If we assume that the system noise is zero, i.e., $\mathbf{C}_k^v = \underline{\mathbf{0}}$, and the involved probability densities are computed exactly, the following holds: First, $\boldsymbol{r}_k^e$ approaches the true radius, due to step 2 and 3 (this is validated by means of simulations in the following section). Actually, this already follows from step 2, but step 3 further improves the estimation result by providing a lower bound for the radius. As a consequence, $\underline{\boldsymbol{p}}_k^e$ approaches the parameter vector of the true circular disc (position and radius). This results from the fact that for given $\underline{\boldsymbol{p}}_k^e$ the special case of known radius is obtained (see Section III-A) and in this case, the set-valued and stochastic uncertainties vanish.

VI. Simulations

In this section, the applicability of the novel method for tracking extended objects is demonstrated by means of simulations. For this purpose, we consider an extended object, whose shape is composed of two overlapping rectangles (see Figure 6a), which could represent an aircraft. The radius of the smallest enclosing circle of the target is 2.

Each measurement source $\tilde{\underline{z}}_{k,j}$ is sampled randomly from these two rectangles and the following three different probability distributions are alternated.

- Measurement sources on the left of the airplane are more likely, which is modeled with the Gaussian mixture

$$0.9 \cdot \mathcal{N}(\underline{x}; \tilde{\underline{x}} - [1.8, 0]^T, \Sigma) + 0.1 \cdot \mathcal{N}(\underline{x}; \tilde{\underline{x}} + [1.8, 0]^T, \Sigma) \ ,$$

- measurement sources on the right of the airplane are more likely, which is modeled with the Gaussian mixture

$$0.1 \cdot \mathcal{N}(\underline{x}; \tilde{\underline{x}} - [1.8, 0]^T, \Sigma) + 0.9 \cdot \mathcal{N}(\underline{x}; \tilde{\underline{x}} + [1.8, 0]^T, \Sigma) \ ,$$

- and measurement sources are uniformly distributed on the airplane,

where $\tilde{\underline{x}}$ denotes the true target center and $\Sigma = \text{diag}(0.05, 0.05)$. In a real-world application, such a scenario could be caused by a target illumination with a radar device from different views of the target object.

The measurement noise $\underline{\boldsymbol{w}}_{k,j}$ is Gaussian with zero mean and covariance matrix $\text{diag}([0.1, 0.1]^T)$. The temporal evolution of the smallest enclosing circle of the extended object is specified by the extended motion model given by Equation (5) with $\mathbf{A}_k = \mathbf{B}_k = \text{diag}([1, 1, 1]^T)$, input $\hat{\underline{u}}_{k-1} = [3, 0, 0]^T$, input noise $\mathbf{C}_k^v = \text{diag}([0.02, 0.02, 0.000001]^T)$, and no set-theoretic error, i.e., $d_k = 0$. The system noise for the radius is quite low in order to model that the radius does not vary over time.

a) Scenario 1: The first scenario demonstrates the benefits of the new approach in comparison to a spatial distribution model [3], [4] . For this purpose, the radius is assumed to be known and only the target center is to be estimated.

The spatial distribution model assumes that the measurement sources are drawn from a uniform distribution on the circle. However, the uniform distribution is approximated with a Gaussian distribution by means of moment matching. By this means, the standard Kalman filter formulas can be used for tracking the center of the target (the target extend is the reflected as an additional additive

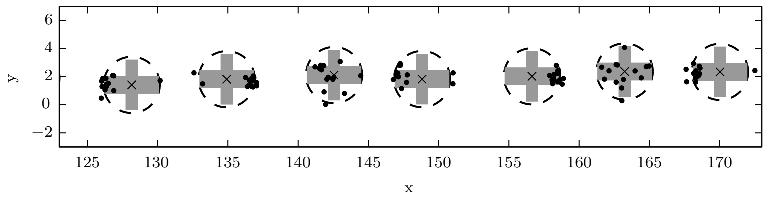

(a) Example trajectory of an extended target: extended target plus its bounding circles (dashed lines) and received measurements (dots).

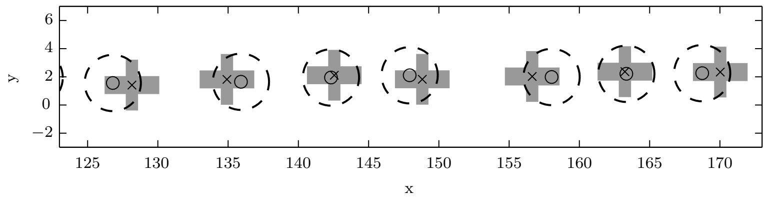

(b) Estimation results for the spatial distribution model (dashed circles) and corresponding 90% confidence ellipses (solid ellipses).

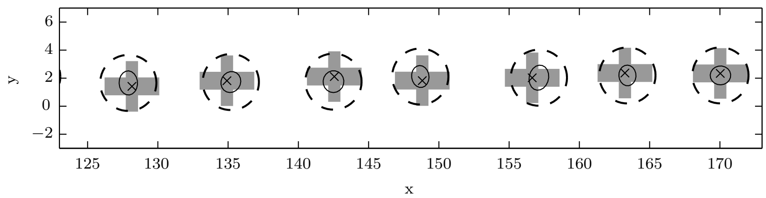

(c) Estimation results for the set-theoretic target extent model (dashed circles) and corresponding 90% confidence ellipses (solid ellipses).

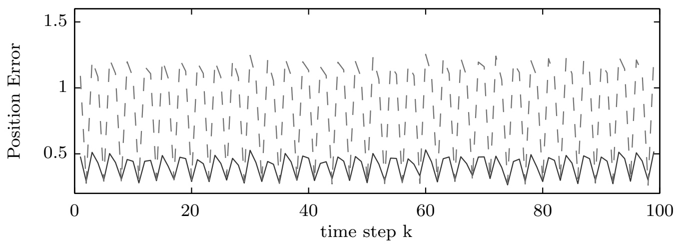

(d) Mean distance between the estimated and true center averaged over 100 simulations runs. Solide line (set-theoretic target model) and dashed line (spatial distribution model).

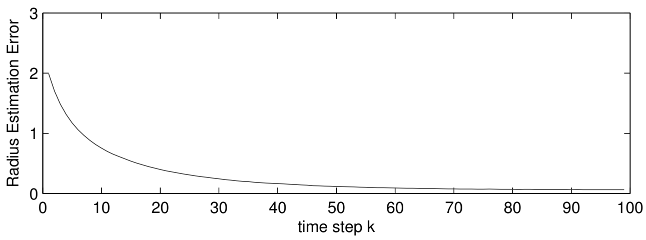

(e) Unknown Radius: Mean distance between the estimated and true radius (averaged over 100 simulations runs).

Fig. 6: Tracking an extended object: Simulation results.

Gaussian noise term). In Figure 6b, the estimation results for an example run for the spatial distribution model are depicted. The results show that the estimates are good, if the measurement sources are uniformly distributed on the target. However, if they are not, poor results are obtained. Even worse, the confidence ellipsoid does not contain the true center of the target. This may cause track loss and results in too small measurement gates.

The estimation results in Figure 6b show that the estimation quality of the SSTE is good no matter what the true distribution of the measurement sources is. And most importantly, the confidence ellipse for the target center does always contain the true target center. The reason is that the new estimator introduced in this work does not make any assumptions on the distribution of the measurement sources. Figure 6d shows the estimation errors for the first 100 time steps averaged over 100 simulation runs for both estimators.

b) Scenario 2: The second scenario shows that the set-theoretic estimator is capable of estimating the radius if it is unknown. For this purpose, the number of measurements n_k produced by the true circular disc with radius r is assumed to be approximately Gaussian distributed, i.e., $n_k \sim \mathcal{N}^*(n_k; 7r, 1^2)$ with an expectation proportional to r. The symbol $\mathcal{N}^*$ denotes the Gaussian distribution with truncated negative values. The a priori distribution of the radius is a Gaussian with mean 5 and variance 0.005. In Figure 6e, the average radius estimation error is plotted for the first 100 time steps. Hence, the radius approaches the true radius.

VII. Generalizations to other Shapes

The combined set-theoretic and stochastic approach for tracking extended objects has been introduced based on circular shapes. The approach has already been used for tracking axis-aligned rectangles in [18]. In case of axis aligned rectangles, the measurement solution sets Δ_k^m are rectangles as well (for known extent). Hence, uncertain rectangles have to be intersected.

In general, the concept can be used for arbitrary target shapes. The target shape determines the measurement solution set. It is then necessary to find a proper conservative approximation for recursive processing of the measurement solution sets. For elliptic target shapes, the approximation techniques introduced in [29] are suitable.

VIII. Conclusions and Future Work

In this article, a novel method for tracking extended objects based on noisy position measurements was presented. In contrast to existing approaches, no assumptions about the location of the measurement sources on the extended object have been made. As a consequence, a combined set-theoretic and stochastic estimation problem is obtained. A particular estimator has been derived for circular discs. In doing so, a novel combined set-theoretic and stochastic estimator that uses random hyperboloids to express the uncertainty about the location and extent of the target object was constructed. Future work will be concerned with extending the proposed method to higher dimensions and other geometric objects such as ellipsoids, arbitrary oriented rectangles or polygons. Finally, methods for incorporating clutter and tracking multiple extended objects will be developed.

REFERENCES

[1] M. J. Waxman and O. E. Drummond, "A Bibliography of Cluster (Group) Tracking," *Signal and Data Processing of Small Targets 2004*, vol. 5428, no. 1, pp. 551–560, 2004.

[2] J. W. Koch, "Bayesian Approach to Extended Object and Cluster Tracking using Random Matrices," *IEEE Transactions on Aerospace and Electronic Systems*, vol. 44, no. 3, pp. 1042–1059, July 2008.

[3] K. Gilholm and D. Salmond, "Spatial Distribution Model for Tracking Extended Objects," *IEE Proceedings on Radar, Sonar and Navigation*, vol. 152, no. 5, pp. 364–371, October 2005.

[4] K. Gilholm, S. Godsill, S. Maskell, and D. Salmond, "Poisson Models for Extended Target and Group Tracking," in *SPIE: Signal and Data Processing of Small Targets*, 2005.

[5] N. Petrov, L. Mihaylova, A. Gning, and D. Angelova, "A Novel Sequential Monte Carlo Approach for Extended Object Tracking Based on Border Parameterisation," in *Proceedings of the 14th International Conference on Information Fusion (Fusion 2011)*, Chicago, Illinois, USA, Jul. 2011.

[6] R. Mahler, "PHD Filters for Nonstandard Targets, I: Extended Targets," in *Proceedings of the 12th International Conference on Information Fusion (Fusion 2009)*, Seattle, Washington, July 2009.

[7] K. Granström, C. Lundquist, and U. Orguner, "A Gaussian Mixture PHD filter for Extended Target Tracking," in *Proceedings of the 13th International Conference on Information Fusion (Fusion 2010)*, Edinburgh, Scotland, Jul. 2010.

[8] A. Swain and D. Clark, "Extended Object Filtering using Spatial Independent Cluster Processes," in *Proceedings of the 13th International Conference on Information Fusion (Fusion 2010)*, Edinburgh, United Kingdom, Jul. 2010.

[9] M. Feldmann, D. Franken, and W. Koch, "Tracking of Extended Objects and Group Targets using Random Matrices," *IEEE Transactions on Signal Processing*, vol. PP, no. 99, p. 1, 2010.

[10] M. Wieneke and W. Koch, "Probabilistic Tracking of Multiple Extended Targets using Random Matrices," in *SPIE: Signal and Data Processing of Small Targets*, vol. 7698, 2010.

[11] M. Baum, M. Feldmann, D. Fränken, U. D. Hanebeck, and W. Koch, "Extended Object and Group Tracking: A Comparison of Random Matrices and Random Hypersurface Models," in *Proceedings of the IEEE ISIF Workshop on Sensor Data Fusion: Trends, Solutions, Applications (SDF 2010)*, Leipzig, Germany, Oct. 2010.

[12] M. Baum and U. D. Hanebeck, "Shape Tracking of Extended Objects and Group Targets with Star-Convex RHMs," in *Proceedings of the 14th International Conference on Information Fusion (Fusion 2011)*, Chicago, Illinois, USA, Jul. 2011.

[13] ——, "Random Hypersurface Models for Extended Object Tracking," in *Proceedings of the 9th IEEE International Symposium on Signal Processing and Information Technology (ISSPIT 2009)*, Ajman, United Arab Emirates, Dec. 2009.

[14] M. Baum, B. Noack, and U. D. Hanebeck, "Extended Object and Group Tracking with Elliptic Random Hypersurface Models," in *Proceedings of the 13th International Conference on Information Fusion (Fusion 2010)*, Edinburgh, United Kingdom, Jul. 2010.

[15] F. Septier, A. Carmi, and S. Godsill, "Tracking of Multiple Contaminant Clouds," in *Proceedings of the 12th International Conference on Information Fusion (Fusion 2009)*, 2009, pp. 1280 –1287.

[16] D. Angelova and L. Mihaylova, "Extended Object Tracking Using Monte Carlo Methods," *IEEE Transactions on Signal Processing*, vol. 56, no. 2, pp. 825–832, Feb. 2008.

[17] M. Baum and U. D. Hanebeck, "Extended Object Tracking based on Combined Set-Theoretic and Stochastic Fusion," in *Proceedings of the 12th International Conference on Information Fusion (Fusion 2009)*, Seattle, Washington, Jul. 2009.

[18] ——, "Tracking an Extended Object Modeled as an Axis-Aligned Rectangle," in *4th German Workshop on Sensor Data Fusion: Trends, Solutions, Applications (SDF 2009), 39th Annual Conference of the Gesellschaft für Informatik e.V. (GI)*, Lübeck, Germany, Oct. 2009.

[19] U. D. Hanebeck and J. Horn, "New Estimators for Mixed Stochastic and Set Theoretic Uncertainty Models: The Scalar Measurement Case," in *Proceedings of the 1999 IEEE Conference on Decision and Control (CDC 1999)*, Phoenix, Arizona, Dec. 1999, pp. 1934–1939.

[20] ——, "A New Concept for State Estimation in the Presence of Stochastic and Set Theoretic Uncertainties," in *Proceedings of the 1999 IEEE/RSJ International Conference on Intelligent Robots and Systems (IROS 1999)*, Kjongju, Korea, Oct. 1999.

[21] U. D. Hanebeck, J. Horn, and G. Schmidt, "On Combining Statistical and Set Theoretic Estimation," *Automatica*, vol. 35, no. 6, pp. 1101–1109, Jun. 1999.

[22] U. D. Hanebeck and J. Horn, "A New Estimator for Mixed Stochastic and Set Theoretic Uncertainty Models Applied to Mobile Robot Localization," in *Proceedings of the 1999 IEEE International Conference on Robotics and Automation (ICRA 1999)*, Detroit, Michigan, May 1999, pp. 1335–1340.

[23] ——, "A New State Estimator for a Mixed Stochastic and Set Theoretic Uncertainty Model," in *Proceedings of SPIE, Vol. 3720, AeroSense Symposium*, Orlando, Florida, Apr. 1999, pp. 336–344.

[24] S. Gollamudi, S. Nagaraj, S. Kapoor, and Y. F. Huang, "Set Membership State Estimation with Optimal Bounding Ellipsoids," in *International Symposium on Information Theory and its Applications (ISITA'96)*, 1996, pp. 262–265.

[25] R. P. S. Mahler, *Statistical Multisource-Multitarget Information Fusion*. Boston, Mass.: Artech House, 2007.

[26] M. F. Huber and U. D. Hanebeck, "Gaussian Filter based on Deterministic Sampling for High Quality Nonlinear Estimation," in *Proceedings of the 17th IFAC World Congress (IFAC 2008)*, vol. 17, no. 2, Seoul, Korea, Jul. 2008.

[27] S. J. Julier and J. K. Uhlmann, "Unscented Filtering and Nonlinear Estimation," in *Proceedings of the IEEE*, vol. 92, no. 3, 2004, pp. 401–422.

[28] D. Simon, *Optimal State Estimation: Kalman, H Infinity, and Nonlinear Approaches*, 1st ed. Wiley & Sons, August 2006.

[29] U. D. Hanebeck and J. Horn, "New Estimators for Mixed Stochastic and Set Theoretic Uncertainty Models: The General Case," in *Proceedings of the 2001 American Control Conference (ACC 2001)*, Arlington, Virginia, 2001.

IX. Appendix

Theorem 1. *Given are a cone* $\underline{\mathbf{C}}(\hat{\underline{z}}_k)$ *and a hyperboloid* $\underline{\mathbf{H}}(\underline{p}^e_{k-1})$. *Furthermore, let*

$$d := \sqrt{(\hat{x}^m_k - x^e_{k-1})^2 + (\hat{y}^m_k - y^e_{k-1})^2}$$

denote the distance between the vectors $[\hat{x}^m_k, \hat{y}^m_k]^T$ *and* $[x^e_{k-1}, y^e_{k-1}]^T$. *If the following condition*

$$d > a^e_{k-1} \tag{6}$$

holds, the hyperboloid $\underline{\mathbf{H}}(\underline{p}_k^e)$ *with*

$$\begin{bmatrix} x_k^e \\ y_k^e \end{bmatrix} = \begin{bmatrix} \hat{x}_k^m \\ \hat{y}_k^m \end{bmatrix} + a_k^e \cdot \tfrac{1}{d}(\begin{bmatrix} x_{k-1}^e \\ y_{k-1}^e \end{bmatrix} - \begin{bmatrix} \hat{x}_k^m \\ \hat{y}_k^m \end{bmatrix}) \text{ and} \tag{7}$$

$$a_k^e = \tfrac{1}{2}(d + \tfrac{(a_{k-1}^e)^2}{d}) \tag{8}$$

has the following properties:

1) *The apex of* $\underline{\mathbf{C}}(\hat{\underline{z}}_k) \cap \underline{\mathbf{H}}(\underline{p}_{k-1}^e)$ *coincides with the apex* $\underline{p}_k^e$ *of* $\underline{\mathbf{H}}(\underline{p}_k^e)$*.*
2) *The intersection of* $\partial\underline{\mathbf{C}}(\hat{\underline{z}}_k) \cap \partial\underline{\mathbf{H}}(\underline{p}_{k-1}^e)$ *is a hyperbola that lies in a plane* E *with normal vector* $[x_{k-1}^e - \hat{x}_k^m, y_{k-1}^e - \hat{y}_k^m, 0]^T$ *and position vector* $\underline{p}_k^e$*.*
3) $E \cap \partial\underline{\mathbf{H}}(\underline{p}_k^e) = \partial\underline{\mathbf{C}}(\hat{\underline{z}}_k) \cap \partial\underline{\mathbf{H}}(\underline{p}_{k-1}^e)$
4) $\underline{\mathbf{C}}(\hat{\underline{z}}_k) \cap \underline{\mathbf{H}}(\underline{p}_{k-1}^e) \subseteq \underline{\mathbf{H}}(\underline{p}_k^e)$

Proof: Can be shown with basic algebraic rules. ■

Remark 5. Condition (6) states that the projection of the apex of $\underline{\mathbf{C}}(\hat{\underline{z}}_k) \cap \underline{\mathbf{H}}(\underline{p}_{k-1}^e)$ onto the $x^c y^c$-plane lies on the segment from $[\hat{x}_k^m, \hat{y}_k^m, 0]^T$ to $[x_{k-1}^e, y_{k-1}^e, 0]^T$. An equivalent condition is the requirement that the r-coordinate of the apex of $\underline{\mathbf{C}}(\hat{\underline{z}}_k) \cap \underline{\mathbf{H}}(\underline{p}_{k-1}^e)$ is greater than a_{k-1}^e.

Definition 3. The function $\mathcal{G}_1 : \mathbb{R}^2 \times \mathbb{R}^3 \to \mathbb{R}^3$ in Equation (4) is defined as follows

$$\mathcal{G}_1(\hat{\underline{z}}_k, \underline{p}_{k-1}^e) = \begin{cases} \mathcal{G}_1^*(\hat{\underline{z}}_k, \underline{p}_{k-1}^e) & \text{if Condition (6) holds} \\ \underline{p}_{k-1}^e & \text{otherwise} \end{cases}$$

where $\mathcal{G}_1^* : \mathbb{R}^2 \times \mathbb{R}^3 \to \mathbb{R}^3$ denotes the total function defined by Equation (7) and (8) that maps $\hat{\underline{z}}_k$ and $\underline{p}_{k-1}^e$ to $\underline{p}_k^e$.

Theorem 2. *Given are a cone* $\underline{\mathbf{C}}(\hat{\underline{z}}_{k,j})$ *and a hyperboloid* $\mathbf{H}(\underline{p}_{k,j-1}^e)$*. Furthermore, let*

$$d := \sqrt{(\hat{x}_{k,j}^m - x_{k,j-1}^e)^2 + (\hat{y}_{k,j}^m - y_{k,j-1}^e)^2}$$

denote the distance between the vectors $[\hat{x}_{k,j}^m, \hat{y}_{k,j}^m]^T$ *and* $[x_{k,j-1}^e, y_{k,j-1}^e]^T$*. If the following condition*

$$d > z_{k,j-1}^e + a_{k,j-1}^e \tag{9}$$

holds, then the hyperboloid $\mathbf{H}(\underline{p}_{k,j}^e)$ *with*

$$\begin{bmatrix} x_{k,j}^e \\ y_{k,j}^e \end{bmatrix} = \begin{bmatrix} \hat{x}_{k,j}^m \\ \hat{y}_{k,j}^m \end{bmatrix} + \tfrac{1}{d}(m z_{apex} + c)(\begin{bmatrix} x_{k,j-1}^e \\ y_{k,j-1}^e \end{bmatrix} - \begin{bmatrix} \hat{x}_{k,j}^m \\ \hat{y}_{k,j}^m \end{bmatrix}) \ , \tag{10}$$

$$z_{k,j}^e = m^2 z_{apex} + mc \ , \tag{11}$$

$$a_{k,j}^e = z_{apex} - z_{k,j}^e \ , \tag{12}$$

where $m = \frac{z^e_{k,j}}{d}$, $c = d + \frac{(a^e_{k,j-1})^2 - (z^e_{k,j-1})^2}{2d}$ *and*

$$z_{apex} = \begin{cases} -\frac{c}{m-1} & \text{if } m^2 - 1 \neq 0 \\ -\frac{c}{2m} & \text{if } m^2 - 1 = 0 \end{cases}$$

has the following properties:

1) *The apex of* $\underline{\mathbf{C}}(\hat{\underline{z}}_{k,j}) \cap \mathbf{H}(\underline{p}^e_{k,j-1})$ *is* $[x^e_{k,j}, y^e_{k,j}, z_{apex}]^T$, *where* $z_{apex} = a^e_{k,j} + z^e_{k,j}$.
2) $\partial\underline{\mathbf{C}}(\hat{\underline{z}}_{k,j}) \cap \partial\mathbf{H}(\underline{p}^e_{k,j-1})$ *is a hyperbola that lies in a plane* E *with normal vector* $[x^e_{k,j-1} - \hat{x}^m_{k,j}, y^e_{k,j-1} - \hat{y}^m_{k,j}, z^e_{k,j}]^T$ *and position vector* $[x^e_{k,j}, y^e_{k,j}, z_{apex}]^T$.
3) $E \cap \partial\mathbf{H}(\underline{p}^e_{k,j}) = \partial\underline{\mathbf{C}}(\hat{\underline{z}}_{k,j}) \cap \partial\mathbf{H}(\underline{p}^e_{k,j-1})$
4) $\underline{\mathbf{C}}(\hat{\underline{z}}_{k,j}) \cap \mathbf{H}(\underline{p}^e_{k,j-1}) \subseteq \mathbf{H}(\underline{p}^e_{k,j})$

Proof: Can be shown with basic algebraic rules. ■

Remark 6. Analog to Condition (6), Condition (9) states that the projection of the apex of $\underline{\mathbf{C}}(\hat{\underline{z}}_{k,j}) \cap \mathbf{H}(\underline{p}^e_{k,j-1})$ onto the $x^c y^c$-plane lies on the segment from $[\hat{x}^m_{k,j}, \hat{y}^m_{k,j}, 0]^T$ to $[x^e_{k,j-1}, y^e_{k,j-1}, 0]^T$.

Definition 4. The function $\mathcal{G}_2 : \mathrm{I\!R}^7 \to \mathrm{I\!R}^4$ is defined as follows

$$\mathcal{G}_2(\hat{\underline{z}}_{k,j}, \underline{p}^e_{k,j-1}) = \begin{cases} \mathcal{G}^*_2(\hat{\underline{z}}_{k,j}, \underline{p}^e_{k,j-1}) & \text{if (9) holds} \\ \begin{bmatrix} \hat{\underline{z}}_{k,j} \\ 0 \end{bmatrix} & \text{if } z^e_{k,j-1} + a^e_{k,j-1} < 0 \\ \underline{p}^e_{k,j-1} & \text{otherwise} \end{cases}$$

where $\mathcal{G}^*_2 : \mathrm{I\!R}^7 \to \mathrm{I\!R}^4$ denotes the total function specified by Equations (10) - (12) that maps $\hat{\underline{z}}_{k,j}$ and $\underline{p}^e_{k,j-1}$ to $\underline{p}^e_{k,j}$.

Marcus Baum received his Dipl.-Inform. in computer science from the the Universitaet Karlsruhe (TH), Germany, in 2007. Currently, he is working towards a PhD degree at the Intelligent Sensor-Actuator-Systems Laboratory, Karlsruhe Institute of Technology (KIT), Germany. His research interests are in the field of extended object and group tracking, nonlinear estimation, and sensor data fusion.

Uwe D. Hanebeck received his Dipl.-Ing. in Electrical Engineering, with first-class honors, from the Ruhr-Universitaet Bochum, Germany, in 1991. He obtained his Dr.-Ing. (Ph.D.) degree in Electrical Engineering from the Technische Universitaet Muenchen, Germany, in 1997. In 2003 he was appointed as professor at the Universitaet Karlsruhe (TH). He is the head of the Intelligent Sensor-Actuator-Systems Laboratory (ISAS), Karlsruhe Institute of Technology (KIT). His research interests are sensor-actuator-networks, human-centered robotics, and telepresence with emphasis on theory-driven approaches based on stochastic estimation theory and uncertainty models. Research results are applied to various fields like human-robot-cooperation, robotic surgery systems, personal assistance systems, and extended-range telepresence.